Sigma J Eng Nat Sci, Vol. 41, No. 2, pp. 344–355, April, 2023

Sigma Journal of Engineering and Natural Sciences
Web page info: https://sigma.yildiz.edu.tr
DOI: 10.14744/sigma.2023.00041

Research Article

Numerical approach of fisher's equation with strang splitting technique using finite element galerkin method

Melike KARTA[1,*]

[1]*Department of Mathematics, Ağrı İbrahim Çeçen University, Ağrı, 04100, Turkiye*

ARTICLE INFO

Article history
Received: 21 November 2021
Revised: 03 January 2022
Accepted: 12 March 2022

Keywords:
Symmetric Strang Splitting; Reaction-Diffusion Equation; Quadratik B-Splines; Finete Element Method

ABSTRACT

In the present paper, non-linear Fisher's reaction-diffusion equation is solved numerically by using Strang splitting technique with the help of Galerkin method combined with quadratic B-spline base functions. For this aim, Fisher's equation is split into two sub-equations with respect to time such that one is linear and the other one is nonlinear. Galerkin method using quadratic B-spline finite elements is applied to each sub-equation. To check the correctness and reliability of the presented approach, we have realized on three numerical examples and have made a comparison with earlier studies existing in the literature calculating the error norms norms L_2 *and* L_∞ .The solutions obtained in the article show that the present method is quite proper for using many partial differential equations in terms of being easy and convenient to computer application.

Cite this article as: Karta M. Numerical approach of fisher's equation with strang splitting technique using finite element galerkin method. Sigma J Eng Nat Sci 2023;41(2):344–355.

INTRODUCTION

The reaction-diffusion equations that play a large role in physical phenomena are widely used in various processes as biological systems, chemical reactions, nuclear reactor physics and population dynamics. Recent studies on these subjects can be given as [1–4].

The commonly known form of the reaction-diffusion equation is defined as in the following form

$$\frac{\partial U}{\partial t} = \lambda \frac{\partial^2 U}{\partial^2 x} + f(U). \quad (1)$$

Here, function f is nonlinear reaction system. U = U(x, t) is a real valued function where t is time, x is space variable. $\lambda \frac{\partial^2 U}{\partial^2 x}$ is the diffusivity term. A special case having the reaction term μ U(1 – U) of equation (1) is presented by

$$\frac{\partial U}{\partial t} = \lambda \frac{\partial^2 U}{\partial^2 x} + f(U). \quad (2)$$

where μ is real parameter. Because Eq.(1) is an equation has multiple uses fields of science and engineering, it has been studied by many researches. Firsty, Fisher [5] used

***Corresponding author.**
*E-mail address: mkarta@agri.edu.tr
This paper was recommended for publication in revised form by Sania Qureshi

Published by Yıldız Technical University Press, İstanbul, Turkey

nonlinear equation (2) to define the propagation of gene in a habitat. The Fisher-Kolmogorov-Petrovsky-Piscunov equation referred to as Fisher KPP equation was investigated by Kolmogoroff *et al.* [6]. For each initial condition of $0 \leq U(x,0) \leq 1$, $-\infty < x < \infty$, they displayed that Fisher's equation (2) has a unique solution bounded for all times, and also found that the problem accepts a progressive wave solution with minimum speed. Canosa [7] discovered that the propagation speed of the waves is linearly proportional to their thickness by phase-plane analysis. Gazdağ and Canosa [8] applied the accurate space derivative (ASD) method. Nonlinear Fisher's equation was studied numerically with help of Petrov-Galerkin finite element method by Tang and Weber [9]. Qiu and Sloan [10] examined the viability of moving mesh method for progressive wave solutions of equation. They showed that progressive wave solution can be used to build a monitor function produced correct solutions by choosing the appropriate mesh method. Zhao and Wei [11] analyzed the approximate solutions of the equation by discrete singular convolution (DSC) algorithm predicted long-time travelling wave behavior. By comparing the numerical results of the (DSC) algorithm with those in the Fourier pseudospectral, the accurate spatial derivates and the Crank-Nicolson schemes, they found that (DSC) algorithm gave better results. The wavelet-Galerkin approach for equation using complex harmonic wavelets have been presented by Cattani and Kudreyko [12]. Mittal and Arora [13] seeked the effective B-spline approximation to solve numerically equation. Dağ *et al.* [14] suggested Galerkin method using quadratic B-spline base functions for equation. To approach the solution of the nonlinear parabolic partial differential equation with Neuman's boundary conditions, Mittal and jain [15] proposed finite element collocation method based on cubic B-spline. Mittal and Jain [16] suggested modified cubic B-spline collocation method for equation. S¸ahin *et al.* [17] developed an efficient B-spline Galerkin scheme for equation. S¸ahin and O¨ zmen [18] performed collocation method with quintic B-spline functions. Ersoy and Dağ [19] used collocation method based on the extended cubic B-spline functions. For solving of Fisher's equation, exponential B-spline collocation method were suggested by Dagğ and Ersoy [20]. Rohila and Mittal [21] applied fourth-order B-spline collocation method to find numerical solution of equation. Tamsir *et al.* [22] suggested an exponential modified cubic B-spline differential quadrature algorithm by using Runge-Kutta method. Dhiman *et al.* [23] used collocation method based on re-defined quintic B-spline with technique the discretion of time derivative Crank-Nicolson(CN). Kapoor *et al.* [24] proposed Hyperbolic B-spline based on differential quadrature method for solving non-linear Fisher's equation.

The present work is summarized as follows: In section 2, Strang splitting method is presented. In section 3, Fisher's reaction diffusion equation is split into two sub-equations and each equation is applied quadratic B-spline Galerkin method. Quadratic B-spline base functions is used for both element shape functions and weight functions. Each sub-problem is coverted into system first order difrential equations and solved with Strang splitting method using Quadratic B-spline Galerkin method. In Section 5, three test problems given with the initial and the boundary conditions are handled. The error norms $L2$ and $L\infty$ are compared with those available in the literature. In Section 6, to emphasize the importance of the present method, a brief conclusion is given. For Eq.(2), the condition given at initial time and conditions given at the boundaries are gotten as

$$U(x,0) = g(x), \qquad x \in [-\infty, \infty] \tag{3}$$

$$\lim_{x\to-\infty} U(x,t) = 1, \ \lim_{x\to\infty} U(x,t) = 0, \tag{4}$$

or

$$\lim_{x\to\pm\infty} U(x,t) = 0. \tag{5}$$

TIME SPLITTING TECHNIQUE

Now it is time to give fundamental concepts lying under the operator splitting methods: First of all, a given complex problem is divided into not only simpler problems but also for smaller time steps. By this way, it is aimed to solve various parts of the problem using and appropriate integration methods [26]. To begin with, we assume that a Cauchy problem is of the following form

$$\frac{dU(t)}{dU} = \Lambda U(t), \qquad U(O) = U_0, t \in [0,T]\,, \tag{6}$$

where $U(x, t)$ is a semi-discretized function given on spatial direction. While applying the splitting technique, the focus will be on states in which the operator $\Lambda = \hat{A} + \hat{B}$ can be expressed as a summation of two linear (and/or nonlinear) operators. Under these conditions, the above equation can be written as

$$\frac{dU(t)}{dU} = \hat{A}U(t) + \hat{B}\,U(t), \qquad U(0) = U_0\,, t \in [0,T]\,, \tag{7}$$

in which the vector U(x, t) represents the solution vector found out using the initial condition $U_0 \in X$, and the operators Λ, $\hat{A}$, $\hat{B}$ are either bounded or unbounded operators defined in a finite or infinite X Banach space. If Lie operator formulation is used, the expression (7) can be rewritten as

$$\frac{dU(t)}{dU} = \hat{A}U(t) + \hat{B}\,U(t), \tag{8}$$

here A and B are Lie operators and $A = \hat{A}(U(t))\frac{\partial}{\partial U}$, $B = \hat{B}(U(t))\frac{\partial}{\partial U}$ order to solve Eq.(8) approximately, the present technique splits the given problem into $\frac{dU(t)}{dt} = AU(t)$ and $\frac{dU(t)}{dt} = BU(t)$ and tries to find the solution either numerically or analitically [27]. When the operators A and Bswap their places and the combination for half time steps are taken as follows

$$S_{\Delta t} = e^{\frac{\Delta t}{2}A} e^{\Delta t B} e^{\frac{\Delta t}{2}A} \text{ or } S_{\Delta t} = e^{\frac{\Delta t}{2}B} e^{\Delta t A} e^{\frac{\Delta t}{2}B}$$

the so-called symmetric Marchuk or more widely known Strang splitting [28] techniques having the schemes $''\mathrm{A}-\mathrm{B}-\mathrm{A}''$ and $''\mathrm{B}-\mathrm{A}-\mathrm{B}''$ are obtained. The procedure for Strang splitting scheme is given as follows

$$\begin{aligned}
&\frac{dU^*(t)}{dt} = AU^*(t),\ U^*(t_n) = U_n^0, \quad t \in [t_n, t_{n+\frac{1}{2}}],\\
&\frac{dU^{**}(t)}{dt} = BU^{**}(t),\ U^{**}(t_n) = U^*\left(t_{n+\frac{1}{2}}\right), \quad t \in [t_n, t_{n+1}],\\
&\frac{dU^{***}(t)}{dt} = AU^{***}(t),\ U^{***}(t_{n+\frac{1}{2}}) = U^{**}(t_{n+1}),\ t \in \left[t_{n+\frac{1}{2}}, t_{n+1}\right],
\end{aligned} \tag{9}$$

where $t_{n+\frac{1}{2}} = t_n + \frac{\Delta t}{2}$ and the aimed solutions are obtained from equation $U(t_{n+1}) = U^{***}(t_{n+1})$. This technique involves an error called splitting error. The local turncation error of this technique

$$T_e = \left(e^{\Delta t(A+B)} - e^{\frac{\Delta t}{2}A} e^{\Delta t B} e^{\frac{\Delta t}{2}A}\right) U(t_n) = \frac{\Delta t^2}{24}\left(2[B,[B,A]] - [A,[A,B]]\right)U(t_n) + O(\Delta t^3)$$

and this indicates to be second-order of present technique.

THE FINITE ELEMENT QUADRATIC B-SPLINE GALERKIN METHOD

Let's first give the B-spline functions before starting the application of the method. Quadratic B-spline functions $\varphi m(x)$ over the solution domain $[XL, XR]$ by the knots xm are described as

$$\varphi_m(x) = \frac{1}{h^3}\begin{cases} (x_{m+2}-x)^2 - 3(x_{m+1}-x)^2 + 3(x_m - x)^2, & [x_{m-1}, x_m]\\ (x_{m+2}-x)^2 - 3(x_{m+1}-x)^2, & [x_m, x_{m+1}]\\ (x_{m+2}-x)^2, & [x_{m+1}, x_{m+2}]\\ 0, & \text{otherwise}\end{cases} \tag{10}$$

in which m = −1, . . . , N. The solution domain for Fisher's equation is restricted over an interval $X_L \le \mathrm{x} \le X_R$. This interval $[X_L, X_R]$ is partitioned into uniformly subintervals $[x_m, x_{m+1}]$ as $x_L = x_0 < x_1 < \cdots < x_N = x_R$ by the nodal point x_m, the mesh size $h = x_{m+1} - x_m$ for m = 0(1) N. The set of quadratic B-splines $\{\varphi_0, \varphi_1, \ldots, \varphi_N\}$ forms a basis over the solution domain $[X_L, X_R]$. A local coordinate system for the finite element $[x_m, x_{m+1}]$ can be submitted with help of transformation $\eta = x - x_m$, $0 \le \eta \le h$, so, we convert quadratic B-spline functions (10) to quadratic B-spline basis functions with form

$$\begin{aligned}
\varphi_{m-1} &= 1 - 2\eta + \eta^2\\
\varphi_m &= 1 + 2\eta - 2\eta^2\\
\varphi_{m+1} &= \eta^2
\end{aligned} \tag{11}$$

The approximate solutions $U_N(x, t)$ on the finite element $[x_m, x_{m+1}]$ is given by

$$U_N(x,t) = \sum_{j=m-1}^{m+1} \delta_m(t)\,\varphi_m(\eta) \tag{12}$$

where δ_{m-1}, δ_m, δ_{m+1} are unknown time dependent parameters and φ_{m-1}, φ_m, φ_{m+1} are element shape functions. At the nodal points x_m, using quadratic B-spline basis functions and the approximate functions (12), the values of U_N and the first order derivative of U_N can be given in terms of the element parameters δ_m by

$$\begin{aligned}
U_m &= U(x_m) = \delta_m + \delta_{m-1}\\
U'_m &= U'(x_m) = \frac{2}{h}(\delta_m - \delta_{m-1})
\end{aligned} \tag{13}$$

Firstly, Eq.(2) is split into two sub-equations with the following form

$$U_t - \lambda U_{xx} - \mu U = 0 \tag{14}$$

$$U_t + \mu UU = 0 \tag{15}$$

To implement the Galerkin method to Fisher's equation, respectively, we multiply all terms in equations (14) and (15) with a weight function W and integrate the resulting equation on the region $[X_L, X_R]$. Thus, we obtain the weak form of equations (14) and (15) as

$$\int_{X_L}^{X_R} W[U_t - \lambda U_{xx} - \mu U]dx = 0 \tag{16}$$

and

$$\int_{X_L}^{X_R} W[U_t + \mu UU]dx = 0 \tag{17}$$

where the weight functions $W(x)$ with approximate functions are gotten as quadratic B-spline functions. Specially, the equations (14) and (15) are valid on the finite element $[x_m, x_{m+1}]$ in form

$$\int_{X_m}^{X_{m+1}} W[U_t - \lambda U_{xx} - \mu U]dx = 0 \tag{18}$$

And

$$\int_{X_m}^{X_{m+1}} W[U_t + \mu UU]dx = 0 \quad (19)$$

respectively. By applying partial integration to the term WU_{xx} in equation (18), we have on integral form needing weaker contiunity property on base functions as follows

$$\int_{X_m}^{X_{m+1}} \left[WU_t + \lambda W_x U_x - \mu WU\right]dx = WU_x \, \mathrm{I}_{x_L}^{x_R} \quad (20)$$

where the first term is zero due to boundary conditions. So, equation (18) is converted into the following form:

$$\int_{X_m}^{X_{m+1}} [WU_t + \lambda W_x U_x - \mu WU]dx = 0 \quad (21)$$

by using $\eta = x - x_m$, transformation, the equations (19) and (21) turn into the following forms

$$\int_0^h \left[WU_t + \lambda W_\eta U_\eta - \mu WU\right] d\eta = 0 \quad (22)$$

$$\int_0^h [WU_t + \mu WUU]d\eta = 0 \quad (23)$$

where the equations (22) and (23) are the element equations for a typical element. Replacing approximation (12) in equations (22) and (23), we obtain the following equations

$$\sum_{j=m-1}^{m+1}[\int_0^h \varphi_i \varphi_j d\eta]\dot{\delta}_j + \lambda \sum_{j=m-1}^{m+1}[\int_0^h \varphi_i' \varphi_j' d\eta]\delta_j - \mu \sum_{j=m-1}^{m+1}[\int_0^h \varphi_i \varphi_j d\eta]\delta_j = 0 \quad (24)$$

and

$$\sum_{j=m-1}^{m+1}[\int_0^h \varphi_i \varphi_j d\eta]\dot{\delta}_j + \mu \sum_{j=m-1}^{m+1} \sum_{k=m-1}^{m+1}[\int_0^h \varphi_i \varphi_j \varphi_k d\eta]\, \delta_k \delta_j = 0 \quad (25)$$

their matrix forms are

$$A^e \dot{\delta}^e + (\lambda B^e - \mu A^e)\delta = 0$$

and

$$A^e \dot{\delta}^e + \mu L^e \delta^e = 0$$

where $\delta^e = (\delta m{-}1,\ \delta m{-}1,\ \delta m{+}1)^T$ is a vector and denote ″. ″ the derivative according to time. Here A^e, B^e, C^e are element matrices introduced in form

$$A^e = \int_0^h \varphi_i \varphi_j d\eta = \frac{h}{30}\begin{bmatrix} 6 & 13 & 1 \\ 13 & 54 & 13 \\ 1 & 13 & 6 \end{bmatrix}$$

$$B^e = \int_0^h \varphi_i' \varphi_j' d\eta = \frac{2}{3h}\begin{bmatrix} 2 & -1 & -1 \\ -1 & -2 & -1 \\ -1 & -1 & 2 \end{bmatrix}$$

$$L^e = \int_0^h \varphi_i \varphi_j \varphi_k d\eta = \frac{h}{3105}\begin{bmatrix} (15,26,1)\delta^e & (26,60,5)\delta^e & (1,5,1)\delta^e \\ (26,60,5)\delta^e & (60,258,60)\delta^e & (5,60,26)\delta^e \\ (1,5,1)\delta^e & (5,60,26)\delta^e & (1,26,15)\delta^e \end{bmatrix}$$

For the purpose of the program, it would be better if L^e matrix is given as $3 \ x \ 3$ dimensional matrix C^e. In this case, it is can be stated bound up with the element parameters δ^e by

$$C^e{}_{ij} = \sum_{k=m-1}^{m+1} L^e{}_{ijk}\, \delta_k{}^e$$

Combining all the element on the domain $[a, b]$, system of differential equations in following form are obtained

$$A\dot{\delta} + (\lambda B - \mu A)\delta = 0 \quad (26)$$

$$A\dot{\delta} + \mu C\delta = 0 \quad (27)$$

Here, $\delta = (\delta_{-1}, \delta_0, \dots, \delta_N)^T$ includes whole the element parameters and A, B and C are band matrices in (26) and (27), if we use the forward difference $\dot{\delta} = \frac{\delta^{n+1} - \delta^n}{\Delta t}$ and Crank-Nicolson formula $\frac{\delta^n + \delta^{n+1}}{2}$ we obtain the following penta-diagonal matrix system, respectively

$$\left[A + (\lambda B - \mu A)\frac{\Delta t}{2}\right]\delta^{n+1} = \left[A - (\lambda B - \mu A)\frac{\Delta t}{2}\right]\delta^n \quad (28)$$

$$\left[A + (\mu C)\frac{\Delta t}{2}\right]\delta^{n+1} = \left[A - (\mu C)\frac{\Delta t}{2}\right]\delta^n \quad (29)$$

In the systems (28) and (29), if the parameters δ_{-1}^{n+1}, δ_N^{n+1} are eliminated using boundary conditions (4), the systems (28) and (29) turn into a penta-diagonal band matrix system $N \ x \ N$. The resulted systems is solved by using Thomas algoriths. The matrix equations (28) and (29) are non-linear because the matrix C depends on parameter δ So, To minimize the non-linearity, two or three times inner iteration in the form of $(\delta^*)^{n+1} = \delta^n + \frac{1}{2}(\delta^{n+1} - \delta^n)$ is applied at each time step.

INITIAL STATE δ^0

The initial vector δ^0 must be calculated from the initial condition and its first order derivative to begin the iteration. It is created $(N+1)x(N+1)$ equation system in form $A^*\delta^0 = B^*$ using the following expression

$$\mathrm{U}(x_m, 0) = g_0(x_m), \quad m = \ 1, \dots, N-1$$

$$U_x(x_L,\ 0) = U_x(x_0, 0) = f_0(0),$$

$$U_x(x_R, t) = U_x(x_N, 0) = f_1(0)\ ,$$

where

$$A^* = \begin{bmatrix} \frac{-2}{h} & \frac{2}{h} & & & \\ 1 & 1 & & & \\ & & \ddots & & \\ & & & 1 & 1 \\ & & & & 1 \quad 1 \end{bmatrix}, \quad \delta^0 = \begin{bmatrix} \delta_0^0 \\ \delta_0^0 \\ \vdots \\ \delta_{N-1}^0 \\ \delta_N^0 \end{bmatrix}, \quad B^* = \begin{bmatrix} U'(x_0) \\ U(x_0) \\ \vdots \\ U(x_{N-1}) \\ U(x_N) \end{bmatrix}$$

The solution of $A^*\delta^0 = B^*$ is obtained by Thomas algorithm.

NUMERICAL EXPERIMENTS AND RESULTS

In this chapter, we will handle three numerical examples commonly existing in literature to Fisher's equation to determine the efficiency of the present method with Strang splitting technique using quadratic B-spline Galerkin method. For this purpose, we compute the error norms L_2 and $L\infty$ and relative error described as

$$L_2 = \|U - U_N\|_2 = \sqrt{h\sum_{j=0}^{N}(U - U_N)^2},$$

$$L_\infty = \|U - U_N\|_\infty = \max_j |U - U_N|\ ,$$

$$\text{Relative error [25]} = \frac{\sqrt{\sum_{j=0}^{N}\left|U_j^{n+1} - U_j^n\right|^2}}{\sqrt{\sum_{j=0}^{N}\left|U_j^{n+1}\right|^2}}.$$

Example 1

Fisher's equation is considered with the initial condition

$$U_0(x) = sech^2(10x)$$

given together with BCs $U(x_L, t) = U(x_R, t) = 0,\ t \geq 0$. Here the reaction and diffusion coefficient is choosen as μ=1 and $\lambda = 0.1$, respectively. For physcial nature of Eq.(2), we have shown various graphical profiles as in study [14] over the region $[-50,50]$. These ones are drawn in Figure 1-3. For values h = 0.025 and Δt = 0.05 and various time level $t = 0$ to $t = 0.5$. Figure 1 shows that near x = 0, U(x, t) reaches maximum value U = 1 but later the peak rapidly comes down since diffusion term U(1-U) dominate over reaction. Because of the influence of reaction, it is indicated the peak value is gradually increasing in time level from t = 0 to 5 in Figure 2. At the same time, it is clearly seen that the peak value reaches until the top U = 1 at times $t = 0(5)40$ in Figure 3. These clarifications can also be cited as studies on [17, 18]. Table 1 presents a comparison of the Relative errors and it indicates that more correct results than [14] studies are obtained.

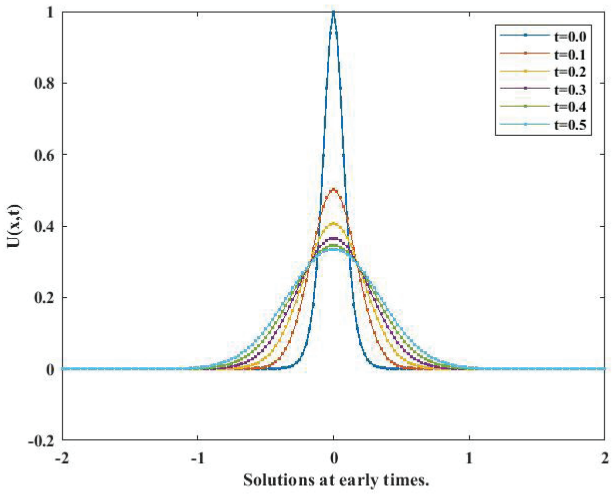

Figure 1. The numerical approaches of Example 1 for t=0 (0.1)0.5.

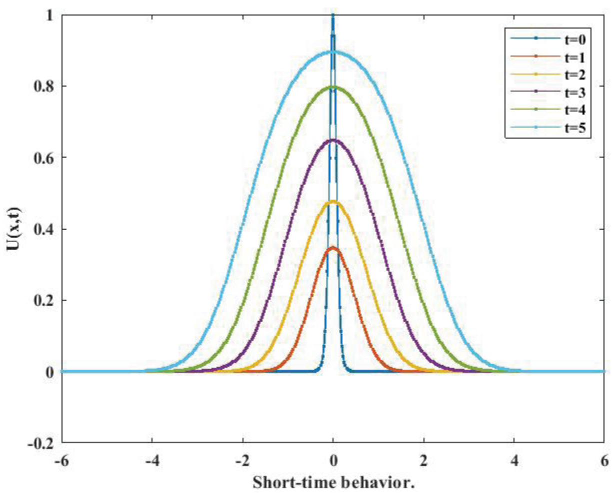

Figure 2. The numerical approaches of Example 1 for t=0 (1)5.

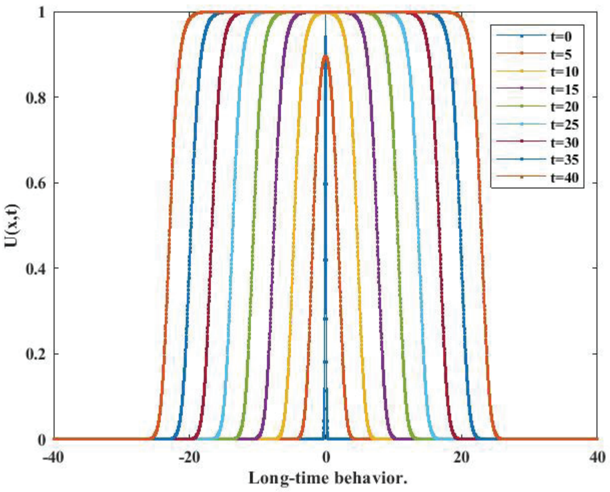

Figure 3. The numerical approaches of Example 1 for t=0(5)40.

4 for values h=0.25, Δt=0.01, t≤ 2. As it is understood from Table 2 and Fig.4 the numerical results obtained with Strang splitting technique using Galerkin finite element method based on quadratic B-spline are fairly better than [15]. Secondly, we take reaction diffusion coefficients μ =10000, λ = 1 respectively, discretization parameters N = 150 and Δt = 0.000005 on the domain [−0.2,0.8]. In Figure 5, it is showed together the analytical solution and the numerical results at times t = 0.0005, 0.001, 0.0015, . . . , 0.0035 and presented graphically the error distribution in Figure 6. Table 3 presents the comparison of the error norms L_2 and $L\infty$ gotten by the present scheme with existing studies in literature. For this, it is choosen as N = 64,150 and Δt = 0.000005 at different time taking into account the references given in Table 3. Additionally, to indicate the credibility and effectiveness of the presented approach, The approximate solution of this problem are shown to compare with analytical solution at various times graphically in Figs 7-8. For this purpose, the parameters are taken μ = 2000 and 5000 for N = 200 with Δt = 0.00001 on the solution region [-0.2,0.8] considering [16] and [24]. As it is known in literature, the approximate solution of equation is unstable in the disturbance wave [14]. To obtain the stable solutions, it is constructed an extra way suggested by Gazdag and Canosa [8]. They have achieved by setting the dispersion equal to zero at each step of time at whole nodal points where it has much smaller values than an empirical threshold value ε, i.e., if

$$U(x_n,t_m) \le \varepsilon \text{ then } U(x_n,t_m) = 0$$

for proposed oscillation problem. We have found that the values ε = $2x10^{-11}$ and ε = $1{,}5x10^{-8}$ for N = 64 and 150 respectively is enough to avoid instability. As it is seen from the Table 3, except for the results FPS [10] and DSC [10] our results appear to be better than the results of other studies. So, the suggested method can be considered as an appropriate approach for numerical solution of other non-linear equations such as the Fisher's equation.

Tablo 1. Comparison of relative errors for Example 1 at various times

Relative Error	t=5	t=10	t=15	t=20	t=40
Present	1.383E – 2	7.835E – 3	6.029E – 3	5.067E – 3	3.417E -3
(Dağ et al., 2010)	1.386E – 2	7.860E – 3	6.054E – 3	5.090E – 3	3.434E -3

Example 2

For this example, we consider Fisher's equation

$$U_t - \lambda U_{xx} - \mu U(1-U) = 0; \ -\infty \le x \le \infty, t \ge 0$$

with initial condition

$$U(x,0) = g_0(x), \ x_L \le x \le x_R$$

and boundary conditions

$$U(x_L,t) = U(x_R,t) = 0.$$

The analytical solution of the this problem is given as

$$U(x,t) = \left[1 + \exp\left(\sqrt{\frac{\mu}{6}}x - \sqrt{\frac{5\mu}{6}}t\right)\right]^{-2}$$

Firstly, we take as λ = 1, μ=2 coefficients of problem and give a comparison between the exact and the approximation solution by calculating the error norms L_2 and $L\infty$ in various times levels for discretization parameters h=1, Δt=0.01 on the region [−10,10], considering study [15]. For this, the graphical profile is drawn in Fig

Tablo 2. Comparison of the error norms L_2 and L_∞ for values $\lambda = 1$, $\mu = 2$ and h = 1, $\Delta t = 0.01$ of Example 2

	Present		**[15]**	
t	L_2	L_∞	L_2	L_∞
0.5	$0.51E-03$	$0.44E-03$	$1.76E-03$	$1.10E-03$
1	$0.47E-03$	$0.25E-03$	$2.92E-03$	$1.75E-03$
1.5	$0.61E-03$	$0.37E-03$	$3.67E-03$	$1.86E-03$
2	$1.96E-03$	$1.88E-03$	$4.50E-03$	$3.00E-03$

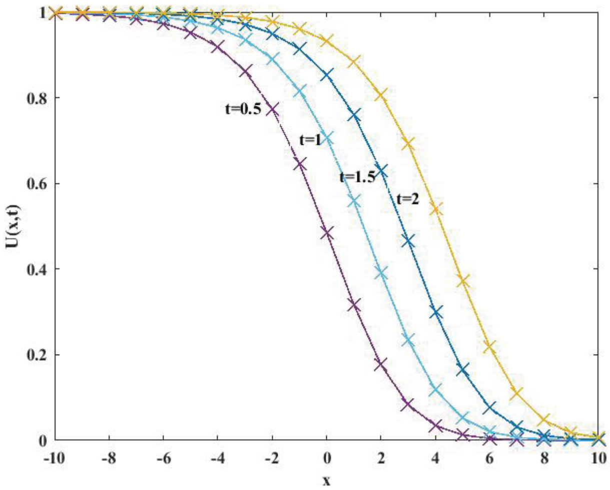

Figure 4. The approximate solutions of Example 2 for $t \le 2$ ($h = 0.25$, $\Delta t = 0.01$).

Table 3. Comparison of the error norms L_2 and $L\infty$ at different times t of Example 2 for $\lambda = 1$, $\mu = 10.000$

Method	**N**	**Error**	**t**			
			0.0005	**0.0015**	**0.0025**	**0.0035**
Present	64	$L2$	$2..39E-4$	$0.01E-1$	$1.48E-2$	$0.38E-1$
		$L\infty$	$0.72E-3$	$0.04E-1$	$0.06E-2$	$1.62E-1$
Present	150	$L2$	$2.13E-4$	$0.03E-2$	$0.12E-2$	$8.28E-3$
		$L\infty$	$0.72E-3$	$0.07E-2$	$0.50E-2$	$3.53E-2$
Dagˇ *et.al.* [14]	64	$L2$	$6.47E-4$	$3.80E-1$	$2.03E-2$	$1.59E-2$
		$L\infty$	$2.55E-3$	$1.62E-1$	$8.65E-2$	$6.98E-2$
Dagˇ *et.al.* [14]	150	$L2$	$6.89E-5$	$1.30E-2$	$1.55E-2$	$8.82E-3$
		$L\infty$	$2.57E-4$	$5.65E-2$	$6.63E-2$	$3.93E-2$
Dağ and Ersoy[19] ($p = 1$)	64	$L\infty$	$1.10E-2$	$1.49E-1$	$3.44E-1$	$5.08E-1$
Dağ and Ersoy[19]	64	$L\infty$	$3.54E-3$ ($p = 3E-6$)	$7.63E-2$ ($p = 1.92E-6$)	$2.04E-2$ ($p = 8.9E-7$)	$1.52E-2$ ($p = 8.9E-7$)
CN [11]	64	$L2$	$1.92E-3$	$2.65E-2$	$6.18E-2$	$9.91E-1$
		$L\infty$	$1.03E-2$	$1.25E-1$	$2.80E-1$	$4.48E-1$
ASD [11]	64	$L2$	$2.09E-3$	$1.06E-2$	$2.02E-2$	$2.35E-2$
		$L\infty$	$1.07E-2$	$4.93E-2$	$9.37E-2$	$9.44E-1$
FPS [11]	64	$L2$	$7.71E-7$	$7.02E-7$	$2.11E-5$	$8.95E-1$
		$L\infty$	$3.13E-6$	$3.90E-6$	$7.82E-5$	$3.42E-1$
DSC [11]	64	$L2$	$1.24E-6$	$5.92E-7$	$1.16E-6$	$1.64E-6$
		$L\infty$	$6.28E-6$	$1.98E-6$	$4.46E-6$	$6.22E-6$

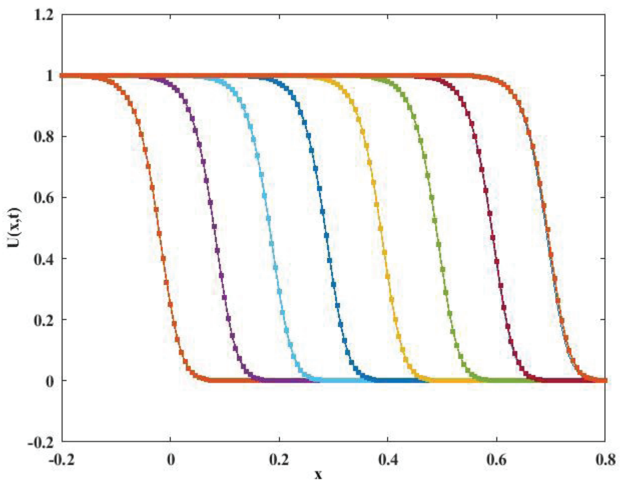

Figure 5. Solution profiles for Example 2.

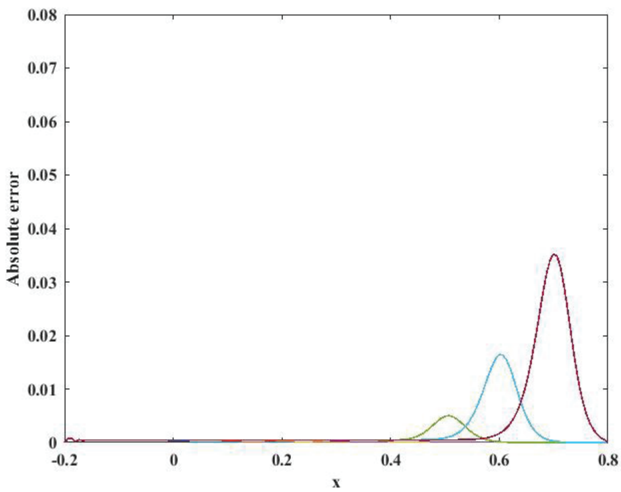

Figure 6. Absolute error distribution for Example 2.

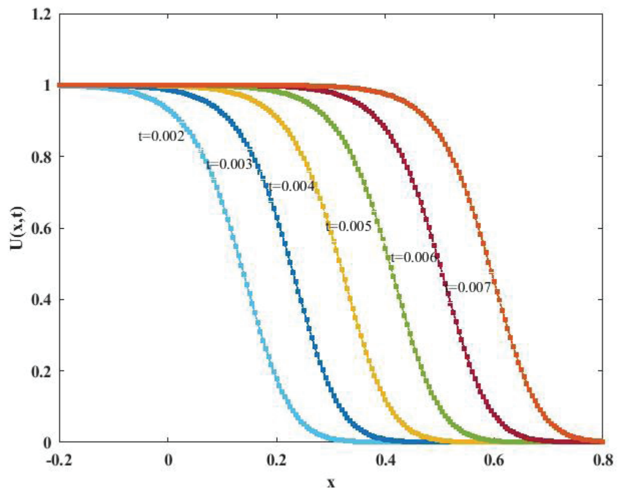

Figure 7. The numerical approaches for $\lambda = 2000$ and $N = 200$ at $t = 0.002$, 0.003,0.004, 0.005, 0.006, 0.007 for Example 2.

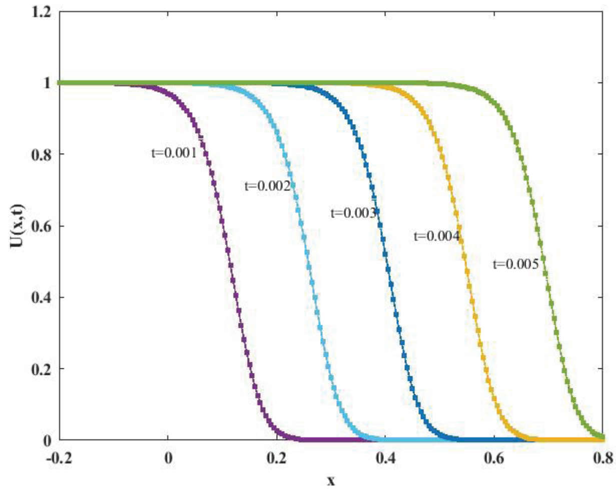

Figure 8. The approximate solutions for $\lambda = 5000$ and $N = 200$ at $t = 0.001$, $t = 0.002$, 0.003,0.004, 0.005 for Example 2.

Example 3

For this example, we take non-linear Fisher's equation given as

$$U_t - \alpha U_{xx} = -\alpha_1 U^2 + \beta_1 U; \ -\infty \le x \le \infty, \ t \ge 0,$$

with the IC

$$U(x,0) = -\frac{\beta_1}{4\alpha_1}\left[sech^2\left(-\sqrt{\frac{\beta_1}{24c}}x\right) - 2tanh\left(-\sqrt{\frac{\beta_1}{24c}}x\right) - 2\right],$$

and BCs

$$U(x_L,t) = 0.5\,, \quad U(x_R,t) = 0.$$

The analytical solution of the equation is taken as

$$U(x,t) = -\frac{\beta_1}{4\alpha_1}\left[sech^2\left(\pm\sqrt{\frac{\beta_1}{24c}}x + \frac{5\beta_1}{12}t\right) - 2tanh\left(\pm\sqrt{\frac{\beta_1}{24c}}x + \frac{5\beta_1}{12}t\right) - 2\right]$$

in solution domain $[-30,30]$. The coefficients found in this problem are choosen as α=1, β_1=0.5, α_1=1, c=1 and the space step h=0.25, time step Δt=0.01 at times t = 2 and t = 4 as in [12], [13], [16]. The comparison with other previous studies of values position and height and absolute error results of the present scheme are given in Table 4-7. These tables shows that our results are very good according the previous results. Figure 9 exhibits approximate and analytical solutions at t = 1(1)5 for parameters h = 0.25, Δt = 0.01 taking into account [13] and [16] and Fig. 9 shows a good compromise between analytical and numerical solutions . Also, with respect [23], we have compared the error norms at t = 1,2,3,4,5 in Table 7 and showed as graphically to together analytical and approximate solution for values h=0.25, Δt=0.01 over domain [−20,20] in Figure 10. Table 8 shows that our results fairly better than [23] and Fig.10 appear to be almost the same of the behavior of analytical and approximate solutions at different times

Table 4. Amplitude and position of the wave at various values of x for t = 2 of Example 3

x	[12]	[13]	Present	Exact
-20	0.498681	0.498653	0.498650	0.498652
-16	0.495130	0.495745	0.495739	0.495740
-12	0.486758	0.486679	0.486668	0.486669
-8	0.459576	0.459478	0.459477	0.459478
-4	0.386681	0.386742	0.386791	0.386791
2	0.158878	0.159011	0.158850	0.158850
6	0.041822	0.041877	0.041851	0.041851
10	0.006455	0.006426	0.006465	0.006465
14	0.000750	0.000746	0.000755	0.000755
18	$7.617E-05$	$7.79E-05$	$7.92E-05$	$7.92E-05$

Table 5. Comparison of absolute error at various values of x for t = 2 of Example 3

x	[13]	[21]	Present
-20	$1.52E-06$	$1.76E-09$	$1.46E-06$
-16	$4.56E-06$	$5.33E-09$	$1.40E-06$
-12	$9.42E-06$	$1.78E-08$	$1.25E-06$
-8	$2.39E-07$	$5.99E-08$	$0.87E-06$
-4	$4.91E-05$	$1.65E-07$	$2.77E-07$
2	$1.61E-04$	$2.28E-07$	$9.24E-08$
6	$2.54E-05$	$1.23E-07$	$0.48E-07$
10	$3.92E-05$	$3.74E-08$	$0.11E-07$
14	$9.46e-06$	$6.18E-09$	$0.02E-07$
18	$1.23E-06$	$7.39E-10$	$0.02E-08$

Table 6. Amplitude and position of the wave at various values of x for t = 4 of Example 3

x	[12]	[13]	Present	Exact
-20	0.498678	0.499412	0.499411	0.499413
-16	0.498525	0.498146	0.498140	0.498142
-12	0.494757	0.494149	0.494138	0.494140
-8	0.481776	0.481763	0.481754	0.481756
-4	0.445508	0.445372	0.445397	0.445398
2	0.279025	0.280082	0.279942	0.279941
6	0.116980	0.117196	0.116963	0.116863
10	0.025927	0.025881	0.025974	0.025974
14	0.003695	0.003559	0.003622	0.003622
18	0.000409	0.000395	0.000406	0.000406

Table 7. Comparison of absolute error at various values of *x* for *t* = 4 of Example 3

x	[13]	[21]	Present
-20	$1.53E-06$	$1.78E-07$	$2.01E-06$
-16	$4.01E-06$	$4.67E-07$	$1.97E-06$
-12	$8.86E-06$	$1.57E-06$	$1.84E-06$
-8	$7.28E-06$	$5.39E-06$	$1.52E-06$
-4	$2.53E-05$	$1.70E-06$	$8.67E-07$
2	$1.41E-04$	$2.74E-06$	$1.17E-07$
6	$2.33E-04$	$4.40E-05$	$1.80E-07$
10	$9.30E-05$	$2.08E-05$	$6.83E-08$
14	$6.29E-05$	$4.86E-06$	$1.34E-08$
18	$1.12E-05$	$6.88E-07$	$0.19E-08$

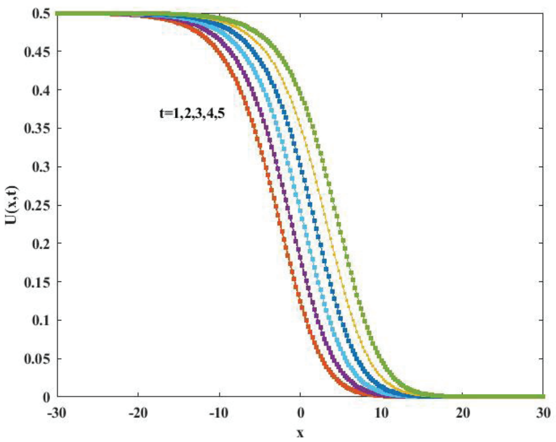

Figure 9. Analytical and approximate solutions at *t* = 1 to 5 for Example 3.

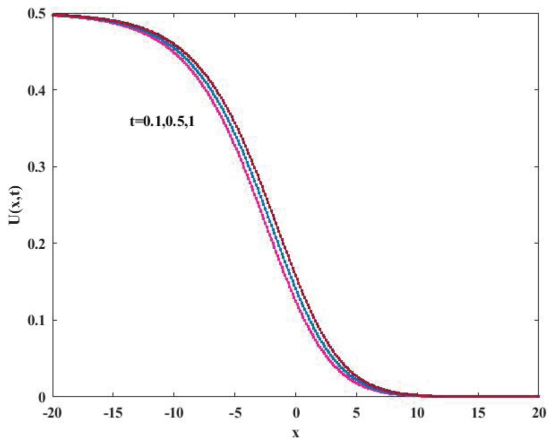

Figure 10. Analytical and approximate solutions at *t* = 0.1, = 0.5, 1 for example 3.

Table 8. The comparison of the error norms L_2 and $L\infty$ for $\Delta t = 0.01$, h = 0.125 on [−20,20] of Example 3

t	Present		[23]	
	L_2	$L\infty$	L_2	$L\infty$
1	$0.9539e-04$	$2.3376e-04$	$1.5509e-04$	$4.1648e-04$
2	$0.9595e-04$	$2.3547e-04$	$2.8126e-04$	$7.5895e-04$
3	$0.9634e-04$	$0.2366e-03$	$3.8053e-04$	$1.000e-03$
4	$0.9661e-04$	$0.2374e-03$	$4.5627e-04$	$1.200e-03$
5	$0.9681e-04$	$0.2379e-03$	$5.1233e-04$	$1.400e-03$

CONCLUSION

In the present work, the approximate solutions of one dimensional Fisher's equation given with convenient the initial-boundary conditions are computed with Strang splitting technique with help of quadratic B-spline Galerkin method. three test problem available in the literature are selected to measure correctness and efficacy of the recommended method. Solutions acquired by the application of the numerical scheme are compared in tables with other studies. From the tables, as it is seen, it is understood that our results are fairly good than existing studies. As a conclusion, we can say that performence of the present method applied for Fisher'equation is very well. Furthermore, Strang splitting techniques combined with cubic B-spline Galerkin method can be successfully applied to nonlinear equations of different types as Fisher's equation in different fields as physics and engineering.

DATA AVAILABILITY STATEMENT

The authors confirm that the data that supports the findings of this study are available within the article. Raw data that support the finding of this study are available from the corresponding author, upon reasonable request.

CONFLICT OF INTEREST

The author declared no potential conflicts of interest with respect to the research, authorship, and/or publication of this article.

ETHICS

There are no ethical issues with the publication of this manuscript.

REFERENCES

[1] Qureshi S, Yusuf A, Aziz S. Fractional numerical dynamics for the logistic population growth model under Conformable Caputo: a case study with real observations. Phys Scr 2021;96:114002. [CrossRef]

[2] Memon Z, Qureshi S, Memon BR. Assessing the role of quarantine and isolation as control strategies faor COVID-19 outbreak: a case study. Chaos Solit Fractals 2021;144:110655. [CrossRef]

[3] Qureshi S, Yusuf A. Fractional derivatives applied to MSEIR problems: Comparative study with real world data. Eur Phys J Plus 2019;134:1–13. [CrossRef]

[4] Qureshi S, Fractal-fractional differentiation for the modeling and mathematical analysis of non- linear diarrhea transmission dynamics under the use of real data. Chaos Solit Fractals 2020;136:109812. [CrossRef]

[5] Fisher RA. The wave of advance of advantageous genes. Ann Eugen 1936;7:355–369. [CrossRef]

[6] Kolmogorov A, Petrovskii I, Piskunov N. Study of a diffusion equation that ıs related to the growth of a quality of matter and ıts application to a biological problem. Moscow Univ Mathem Bull 1937;1:1–26.

[7] Canosa J. On a nonlinear diffusion equation describing population growth. J Res Dev 1973;17:307–313. [CrossRef]

[8] Gazdag J, Canosa J. Numerical solution of Fisher's equation. J Appl Prob 1974;11:445–457. [CrossRef]

[9] Tang S, Weber RO. Numerical study of Fisher's equation by a Petrov-Galerkin finite element method. J Austral Math Soc Ser B 1991;33:27–38. [CrossRef]

[10] Qiu Y, Sloan DM. Numerical solution of Fisher's equation using a moving mesh method. J Comput Phys 1998;146:726–746. [CrossRef]

[11] Zhao S, Wei GW. Comparison of the discrete singular convolution and three other numerical schemes for solving Fisher's equation. J Sci Comput 2003;25:127–147. [CrossRef]

[12] Cattani C, Kudreyko A. Mutiscale analysis of the fisher equation. Lect Notes Comput Sci 2008;5072: 1171–1180. [CrossRef]

[13] Mittal RC, Arora G. Efficient numerical solution of Fisher's equation by using B-spline method. Int. J Comput Math 2010;87:3039–3051. [CrossRef]

[14] Dagg II, Sahin A, Korkmaz A. Numerical investigation of the solution of Fisher's equation via the B-spline Galerkin method. Numer Methods Partial Differ Equ 2010;26:1483–1503. [CrossRef]

[15] Mittal RC, Jain R. Cubic B-splines collocation method for solving nonlinear parabolic partial differential equations with Neumann boundary conditions. commun Nonlinear sci. Numer.Simulat 2012;17:4616–4625. [CrossRef]

[16] Mittal RC, Jain RK. Numerical solutions of nonlinear Fisher's reaction-diffusion equation with modified cubic B- spline collocation method. Math Sci 2013;7:1–10. [CrossRef]

[17] Sahin A, Dagg II, Saka B. A B-spline algorithm for the numerical solution of Fisher's equation. Kybernetes 2008;37:326–342. [CrossRef]

[18] Sahin A, Ozmen O. Usage of higher order B-splines in numerical solution of Fishers equation. Int J Nonlinear Sci 2014;17:241–253.

[19] Ersoy O, Dagg I.. The extended B-spline collocation method for numerical solutions of Fishers equation. AIP Conf Proc 2015;1648:370011. [CrossRef]

[20] Dag I, Ersoy O. The exponential cubic B-spline algorithm for Fisher equation. Chaos Solit Fractals 2016;86:101–106. [CrossRef]

[21] Rohila R, Mittal R.C. Numerical study of reaction diffusion Fisher's equation by fourth order cubic B-spline collocation method. Math Sci 2018;12:79–89. [CrossRef]

[22] Tamsir M, Srivastava VK, Dhiman N, Chauhan A. Numerical computation of nonlinear fisher's reaction-diffusion equation with exponential modified cubic b-spline differential quadrature method. Int. J Appl Comput Math 2018;4:1–13. [CrossRef]

[23] Dhiman N, Chauhan A, Tamsir M, Chauhan A. Numerical simulation of Fisher's type equation via a collocation technique based on re-defined quintic B-splines. Multidiscip Model Mater Struct 2020;16:1117–1130. [CrossRef]

[24] Kapoor M, Joshi V. Solution of non-linear Fisher's reaction-diffusion equation by using Hyper- bolic B-spline based differential quadrature method. J Phys Conf Ser 2020;1531:012064. [CrossRef]

[25] Madzvamuse A. Time stepping schemes for moving grid finite elements applied to reaction- diffusion systems on fixed and growing domains. J Comput Phys 2006;214:239–263. [CrossRef]

[26] Hundsdorfer W, Verwer J. Numerical solution of time-dependent advection-diffusion- reaction equations . 1st ed. Berlin: Springer; 2003. [CrossRef]

[27] Seydaogglu M, Blanes S. High-order splitting methods for separable non-autonomous parabolic equations. Appl Numer Math 2014;84:22–32. [CrossRef]

[28] Strang G. On the construction and comparison of difference schemes. J Numer Anal 1968;5:506–517. [CrossRef]